

# Hydration state of gelatine studied by Time Domain Nuclear Magnetic Resonance (TD-NMR): a preliminary study

M. C. Vachier & D. N. Rutledge

*Institut National Agronomique Paris-Grignon, Laboratoire de Chimie Analytique, 16 rue Claude Bernard, 75231, Paris Cedex 05, France*

(Received 21 July 1995; revised version received 19 October 1995; accepted 19 October 1995)

Hydration state was studied by time domain nuclear magnetic resonance (TD-NMR) in order to characterize water associated with macromolecules such as gelatine. In a first experiment, transverse water proton relaxation rates ( $R_2$ ) of water-rich samples were measured at different temperatures. The pH of gelatine solutions was adjusted with NaOH.  $R_2$  shows characteristic dispersion as a function of Carr-Purcell-Meiboom-Gill (CPMG) interpulse spacing. Moreover, the more dilute the gelatine, the less structured the gelatine sol and the slower the relaxation.

For water-poor gelatines (0 to 66% water, wet basis), the longitudinal relaxation time ( $T_1$ ), the transverse relaxation time ( $T_2$ ) and the free induction decay (FID) were measured and the ratio of the initial amplitude of the slow relaxing  $T_2$  components to the amplitude of the FID signal at 11  $\mu$ s ( $M_{0,src}/FID_{11}$ ) was calculated. These NMR curves and calculated values were also studied by means of multivariate statistical analysis to determine which parameters were the best predictors of moisture content and water mobility. Copyright © 1996 Elsevier Science Ltd

## INTRODUCTION

Water determination in food products is of major importance because their quality (texture, structure, fitness to transformation, etc.) and stability (microbial growth, storage, deterioration, etc.) largely depend on its physical state (Duckworth, 1975). It is therefore essential, both for the agrofood industry and for researchers, to develop simple and efficient methods to quickly monitor the hydration state of biological products.

The relaxation curves and calculated relaxation times obtained by time domain nuclear magnetic resonance (TD-NMR) directly give information about the mobility of the protons in the sample, and so may be correlated with various factors such as water content, water mobility and solute concentration (Belton, 1984).

Gelatine was chosen for this study because it is a good model for food products and its gels have remarkable mechanical properties. In a first experiment, we studied the influence of factors such as water content, pH of gelatine and analysis temperature on relaxation phenomena. In a second experiment, we analysed the behaviour of NMR parameters as a function of water content.

The data obtained give information about the structure of the gelatines, their hydration state and the

nature of the interactions between water and the macromolecules. Finally, these studies help pinpoint NMR parameters which may be used as sensitive probes of water content and hydration state.

## MATERIALS AND METHODS

### Water content determination

The moisture contents of the gelatine powder (Prolabo, No. 24 350.262) and of the prepared samples were measured by weight loss after drying for 24 h at 106°C. Results are expressed on a wet basis.

### Sample preparation

Water-rich gelatines (from 70 to 80% water) were prepared by adding gelatine powder to water containing 0.05% sodium azide as an antimicrobial agent. pH (6, 7 and 8) was adjusted with NaOH (1 N). NMR tubes (10 mm external diameter) were then filled to 1 cm height, sealed and maintained at 4°C.

Water-poor gelatines were prepared from a 70% water gelatine; 0.5-cm cubes were dried at 30°C in hermetically sealed jars containing saturated NaOH. Cubes

were removed at different times to obtain a broad range of water concentrations, from 0 to 66%. NMR tubes were filled to 3 cm height and sealed to avoid microbial development. Sample height was increased for these gelatines to compensate for lower signal intensities due to low water contents.

### NMR measurements

All NMR measurements were carried out on a 20 MHz Minispec pc120 (Bruker) with an audio filter bandwidth of 1 MHz and a phase sensitive detector.

#### Water-rich gelatines

Measurements were done on samples at 10°C, 20°C and 40°C.

**Transverse relaxation rate ( $R_2$ )** In order to estimate the influence of chemical exchange on  $R_2$ , transverse relaxation curves were acquired using a Carr–Purcell–Meiboom–Gill (CPMG) sequence with variable inter-pulse spacings (Table 1). This sequence can be schematized as follows:

$$\begin{array}{l} 90^\circ - \text{tau} - \{[180^\circ - 2\text{tau}]M \\ 180^\circ - \text{tau} - \text{measurement} - \text{tau}\}N \end{array}$$

where 2tau is the interpulse delay.

The relaxation curves were all of the same total duration and had 56 time points in common. The duration of these CPMG curves allows a correct characterization of the slow relaxing components (water protons and exchangeable gelatine protons).

A non-linear regression program based on the Marquardt algorithm (Marquardt, 1963) was used to decompose the different relaxation curves into sums of exponentials.

#### Water-poor gelatines

Since we wished to study these samples in the gel state and since the cubes which have a higher moisture content may melt above 30°C, all measurements were carried out at 20°C. Tubes were thermostated at 20°C for 1 h prior to analysis. Instrument adjustment was performed on every tube to eliminate instrumental artefacts which could result from variations in water content.

Table 1. Characteristics of the CPMG sequences used

Total duration (ms)	2tau (ms)	M	N
1680	1.25	7	168
1680	1.875	7	112
1680	2.5	3	168
1680	3.75	7	56
1680	3.75	3	112
1680	5	1	168
1680	7.5	3	56
1680	7.5	1	112
1680	15	1	56

**Free induction decay** The decrease in the free induction decay (FID) was measured between 11  $\mu$ s and 107  $\mu$ s after a 90° pulse.

**Longitudinal relaxation time ( $T_1$ ) and transverse relaxation time ( $T_2$ )** Classical sequences such as CPMG for  $T_2$  ( $1/R_2$ ) or Inversion-Recovery for  $T_1$  ( $1/R_1$ ) can not be used for water-poor samples. The liquid concentration is so low that the FID decreases very quickly and after about 70  $\mu$ s no signal is detected. The 90°– $t$ –90° pulse sequence used allows simultaneous estimation of  $T_1$ ,  $T_2$  slow relaxing component ( $T_{2\text{src}}$ ) and its initial amplitude ( $M_{0\text{src}}$ ) (Monteiro Marques *et al.*, 1991). In fact, this sequence involves an FID and a progressive saturation. If we designate  $\text{FID}_x$  as the amplitude of the signal  $x$   $\mu$ s after the first 90° pulse, the slope of the plot of the logarithm of  $\text{FID}_x$  as a function of  $x$ , for  $x=42$   $\mu$ s and  $x=73$   $\mu$ s, may be considered equal to  $-R_{2\text{src}}$  ( $=-1/T_{2\text{src}}$ ).  $M_{0\text{src}}$  is the exponential of the intersection at the origin. In the same way, if  $M_t$  represents the amplitude of the signal 11  $\mu$ s after the 90°– $t$ –90° sequence, the slope of the plot of the logarithm  $[(\text{FID}_{11}-M_t)/\text{FID}_{11}]$  as a function of  $t$ , for  $t=7$  ms and  $t=70$  ms, was considered equal to  $-R_1$  ( $=-1/T_1$ ). Measurements were done at 11  $\mu$ s after the sequence and not at 70  $\mu$ s because preliminary experiments had revealed that, at 20°C, the behaviour can be considered as monoexponential (the short  $T_1$  component only represents 5% of the total population). The times chosen are those which give the greatest variability for the different water contents. In order to correct for variations in sample size,  $M_{0\text{src}}/\text{FID}_{11}$  was calculated for each sample.

## RESULTS AND DISCUSSION

### Water-rich gelatines

#### 40% Sol form

Decomposition of the CPMG curves reveals the existence of two components. For the slow relaxing component (water and exchangeable protons of gelatine), a decrease in  $R_2$  values ( $=1/T_2$ ) with tau being the delay between the 90° pulse and the 180° pulse as schematized in NMR measurement section is observed (Fig. 1).

This corroborates the hypothesis of Hills *et al.* (1990) concerning a transition between a system where the chemical exchange is important and a system where it is negligible (Carver & Richard, 1972; Hills *et al.*, 1990). When tau is long compared to the exchange rate, this exchange may dephase the spins and enhance relaxation. On the other hand, when tau is short, there is no time for exchange to occur and relaxation rates are lower. According to these authors, at pulse spacings that are long compared with the exchange lifetime, and provided that the fraction of exchangeable protons,  $P_b < 1$ ,  $R_2$  is given by:

$$R_2 = R_{2w} + P_b k_b \left\{ \frac{R_{2b}^2 + R_{2b} k_b + (\delta\omega)^2}{(R_{2b} + k_b)^2 + (\delta\omega)^2} \right\}$$

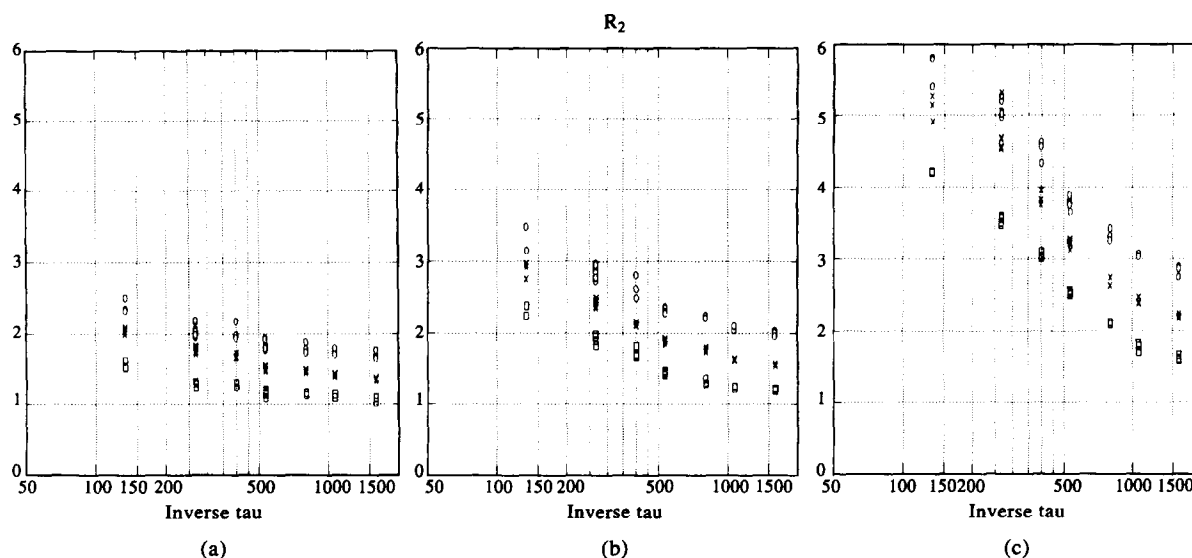


Fig. 1. Effect of water content on the dispersion of  $R_2$  at 40°C at (a) pH 6, (b) pH 7 and (c) pH 8. ○, gelatine 70% water; ×, gelatine 75% water; □, gelatine 80% water

where  $R_{2w}$  is the relaxation rate for bulk water,  $k_b$  the exchange rate,  $R_{2b}$  the relaxation rate of the exchangeable solute protons and  $\delta\omega$  the chemical shift difference between these protons and water.

To the contrary, when the interpulse delay is shortened,  $R_2$  decreases to the limit where the chemical shift terms are no longer effective:

$$R_2 = R_{2w} + \frac{P_b}{\left(\frac{1}{k_b} + \frac{1}{R_{2b}}\right)}$$

if  $k_b \gg R_{2b}$  then  $R_2 = R_{2w} + P_b R_{2b}$

if  $k_b < R_{2b}$  then  $R_2 = R_{2w} + P_b k_b$

As can be seen in Fig. 1, the more concentrated and the more basic the gelatine, the higher all the  $R_2$  values. Moreover, the  $R_2$  dispersion is greatest at pH 8 (Fig. 1c). At different pHs, an increase in water content does not have the same effect on  $R_2$ . At pH 8, gelatines at 75% are closer to those at 70% than to those at 80%. However, an increase in water content for a given pH does not appreciably alter the dispersion curvature of the  $R_2$  (Fig. 1).

The basification causes either an increase in the rate of proton exchange ( $k_b$ ) between water and gelatine or a greater difference in the chemical shifts ( $\delta\omega$ ) of the water and the gelatine, resulting in an increase in the  $R_2$  dispersion.

The increase in the charge of the protein can also explain the increase in the  $R_2$  with pH. The protein being more charged, its rigidity may increase due to electrostatic repulsion. Since the exchange is going on between the water protons and the gelatine protons, this might be reflected by an overall increase in  $R_2$ .

The fact that  $R_2$  increases with pH, for all water contents, even at very short values of tau indicates either that the intrinsic relaxation rate ( $R_{2b}$ ) or the exchange rate ( $k_b$ ) are greater at higher pH. This increase in  $R_{2b}$

and/or  $k_b$  must be sufficiently great to compensate for the decrease in the number of exchangeable protons ( $P_b$ ) under basic conditions.

#### 10°C and 20°C: gel form

The relaxation at these temperatures is mono-exponential. The water mobility having decreased, its  $R_2$  is closer to that of gelatine, making them more difficult to distinguish. Since diffusion is not very great, we expect to observe a decrease in the  $R_2$  dispersion. In fact, no obvious dispersion is observed, except a very slight one at 20°C for gelatines at 80% water (Fig. 2).

The lower the water content and the higher the pH, the greater the  $R_2$ . The same observations, as for 40°C, can be made for these temperatures as far as the effects of pH and water concentration are concerned: gelatines at 75% water are closer to those at 70% than to those at 80% (Fig. 2a-c), and  $R_2$  increases with the pH, even for the very short tau.

At 20°C, there is a difference in the behaviour of the curves as a function of water concentration. The increase in water concentration from 70% to 75% significantly changes the  $R_2$  only at pH 6, whereas from 75% to 80% the  $R_2$  values change for all three pHs. This results in a greater difference between the  $R_2$ s at pH 6 and pH 7 for 75% water than for the other water contents (Fig. 2b). On the other hand, the  $R_2$  increase from pH 7 to pH 8 is the same for all water concentrations.

At 10°C, the more basic the pH, the more the gel at 80% differs from the 70% and the 75% gels. At pH 7, there is an inversion of  $R_2$  between the gel at 70% and the gel at 75%. Indeed, the former has an  $R_2$  slightly greater than the latter. This tendency increases with the pH (data not shown).

At a given pH, addition of water decreases the gelatine  $R_2$ . Going from 70% to 75% at pH 6 gives an important decrease in  $R_2$  whereas it increases the  $R_2$  at pH 7. This observation and the inversion of  $R_2$  are in

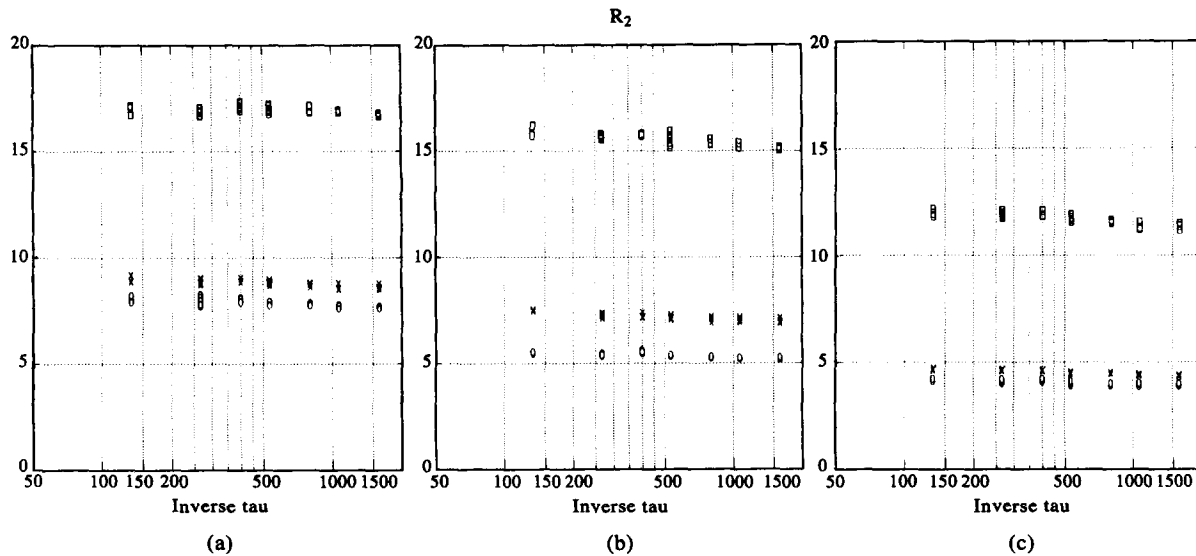


Fig. 2. Effect of pH on  $R_2$  at 20°C for gelatines with 70% (a), 75% (b) and 80% water (c).  $\circ$ , pH 6;  $\times$ , pH 7;  $\square$ , pH 8.

favour of the existence of a critical pH above which adding water will decrease  $R_2$ . According to these results, this value would be located between pH 6 and pH 7 and could be the  $pH_i$  of the gelatine (data not shown). To test this hypothesis, electrophoresis and electrofocalization have been carried out under denaturing conditions. These experiments were, however, inconclusive as the bands were very overlapped and smeared. Other analyses such as turbidity measurements or even electrofocalization on more homogeneous and pure gelatines are being carried out in order to determine this particular pH value.

The effect of the temperature on water mobility is important. At 40°C, gelatine gels are in the sol form and two relaxation components are observed. On the other hand, at 10 and 20°C they are in the gel form and present a single component. One can suppose the existence of a critical temperature (i.e. melting point), between 20 and 35°C, at which there is a transition from a biexponential to a monoexponential system. It is to be noted that, although water mobility and gelatine structure are different at 40 and at 10°C, the shorter  $R_2$ s at 40°C are equal to the monoexponential  $R_2$ s at 10°C (data not shown).

#### Water-poor gelatine

Calculated NMR parameters ( $T_1$ ,  $T_{2\text{src}}$ ,  $M0_{\text{src}}/FID_{11}$ ) and normalized FID intensities were plotted against water content.  $M0_{\text{src}}/FID_{11}$  increases with the water content with a sudden increase at about 20% (Fig. 3). The shape of these curves supports the hypotheses of Monteiro Marques *et al.* (1991) based on their study on the drying of carrots:

1. Below 20%, water molecules are strongly associated with the solid matrix and so do not initially contribute to the signal of the slow relaxing components. This explains why the signal of the slow

relaxing components is weak. As the water content increases, the water  $T_2$  increases, leading to a rapid increase in  $M0_{\text{src}}/FID_{11}$ .

2. Near 20%, either water associated with macromolecular fragments starts to plasticize them, causing the proportion of slow relaxing components to increase more than expected for the quantity of water added, or solutes are dissolved, similarly leading to an extra increase in the proportion of slow relaxing components.  $^{23}\text{Na}$ -NMR analyses will be performed to test this hypothesis.
3. Beyond 25%, the water  $T_2$  no longer changes significantly with water content, the solutes are all dissolved and no increase in macromolecular mobility is possible. The slow linear increase in  $M0_{\text{src}}/FID_{11}$  is then solely due to the extra water molecules introduced.

Principal component analysis (PCA) was carried out both on the NMR parameters ( $M0_{\text{src}}/FID_{11}$ ,  $T_{2\text{src}}$  and

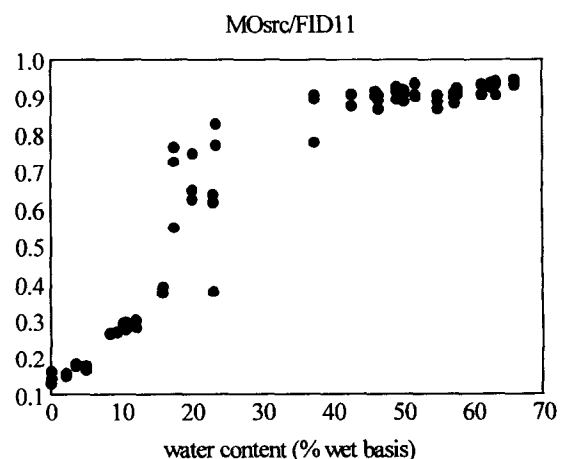


Fig. 3. Initial signal amplitude of the slow relaxing protons divided by the amplitude of the FID signal at 11  $\mu\text{s}$ , as a function of the water content.

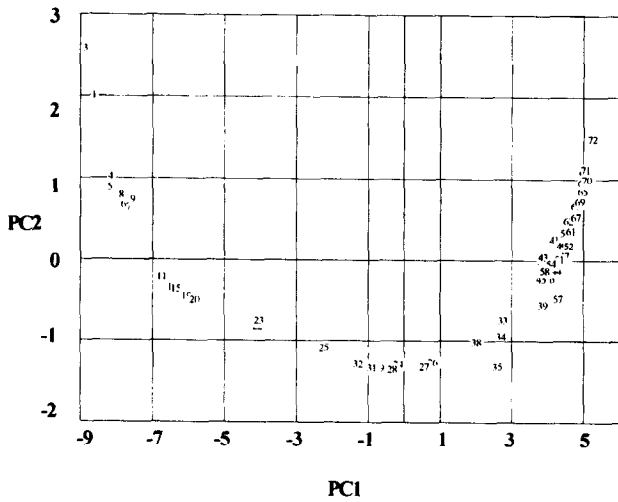


Fig. 4. Plot of the first principal components (96.3% and 3% of variance). Objects are numbered in order of increasing water content.

$T_1$ ) and on the raw data (FID values) using the Unscrambler (CAMO, Trondheim, Norway). PCA does not assume any *a priori* model, it simply visualizes the sources of variability in the data. The PCA reveals that samples are classified according to water content along Principal Component 1 (PC1) (Fig. 4). The variables which contribute most to PC1 are  $T_{2\text{src}}$ ,  $M0_{\text{src}}/FID_{11}$  and the points on the FID curve (Fig. 5). These vari-

ables are therefore all indicative of the increase in water content. PC2 is due almost exclusively to  $T_1$ . Gelatines at very low and very high water contents therefore have higher  $T_1$  values than intermediate ones. This is explained by the fact that, when the movements are rather slow (solids) or fast (liquids), the return to equilibrium takes longer.

As  $T_{2\text{src}}$ ,  $M0_{\text{src}}/FID_{11}$  and  $T_1$  are the variables which give the most relevant information about the water content and the hydration state of gelatine, we found it judicious to plot these parameters one against another. These NMR parameters are influenced by the dynamics of the water molecules which vary not only with the water content but also with the interactions between the water molecules and the matrix. Variability in these interactions from sample to sample may be at the origin of the dispersion of the points in the plots of NMR parameters versus water content. Plotting the parameters one against the other should therefore compensate for the variations. This was successful in so far as all these curves were smoother than those with water content as the abscissa (data not shown).

Thus the plot of  $T_1$  against  $M0_{\text{src}}/FID_{11}$  shows a smooth parabolic curve with a minimum at approximately (0.5, 50 ms) (Fig. 6). It is noteworthy that this minimum, which takes place when 50% of the signal is due to slow relaxing components, corresponds to the inflexion point of the plot of  $M0_{\text{src}}/FID_{11}$  against water content (Fig. 3).

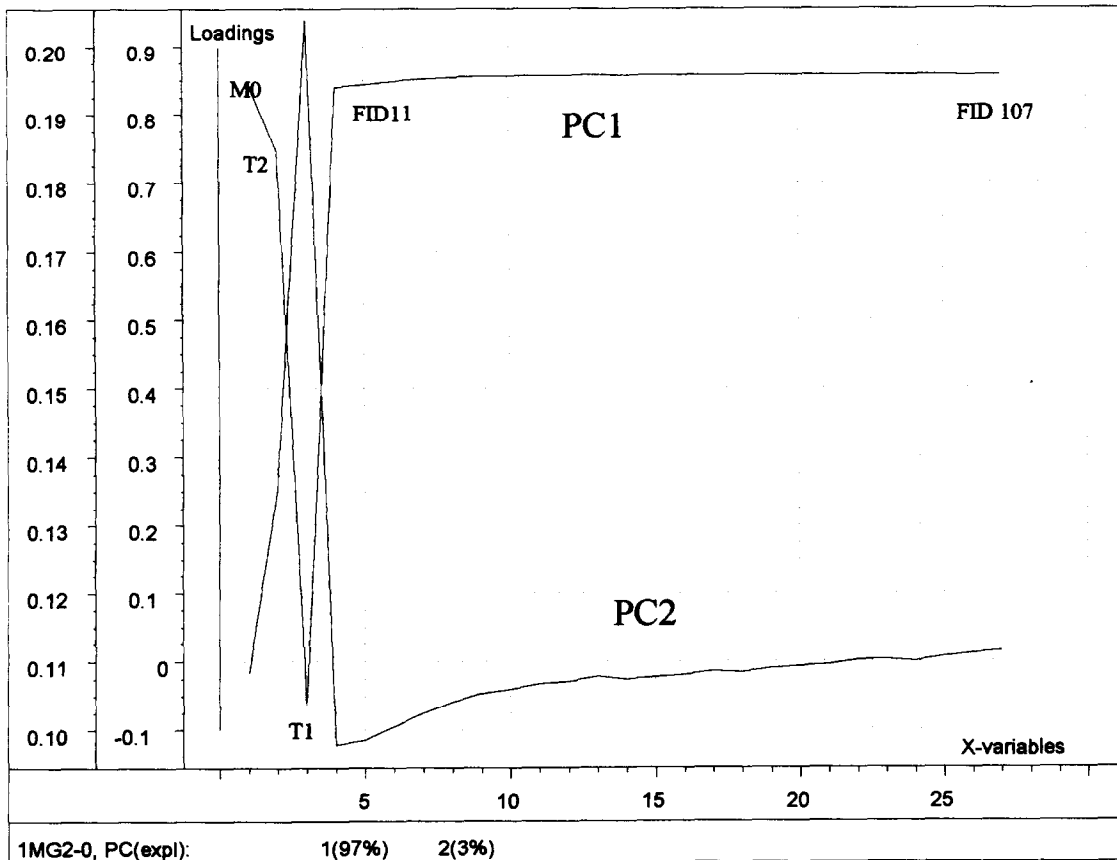


Fig. 5. Loadings of the  $M0_{\text{src}}/FID_{11}$ ,  $T_2$ ,  $T_1$  and FID points for PCA.

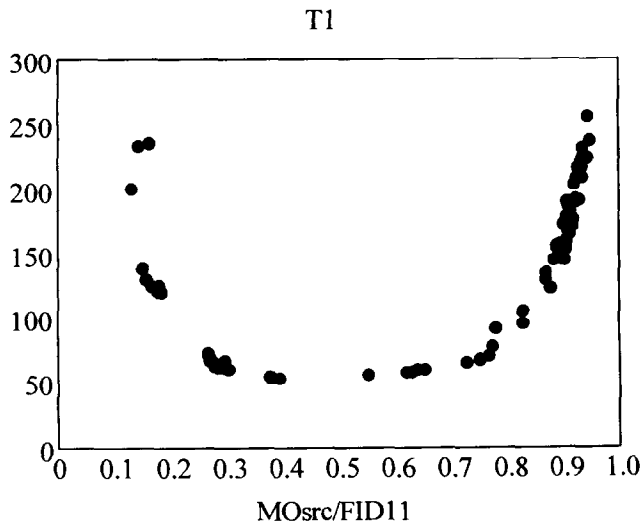


Fig. 6. Longitudinal relaxation time,  $T_1$ , as a function of the initial amplitude of the slow relaxing components divided by the FID amplitude at 11  $\mu$ s ( $MO_{src}/FID_{11}$ ).

As we have shown above, FID points contribute to PC1 and the samples are classed along this axis with increasing water contents. In order to determine the nature of the relationship between the FID signal and water content, a partial least squares (PLS1) regression was performed between the normalized FID points and the water content. The major contribution to PC1 (99% of the total variability) is from the points beyond 27  $\mu$ s (mobile water protons) whereas PC2 is mainly influenced

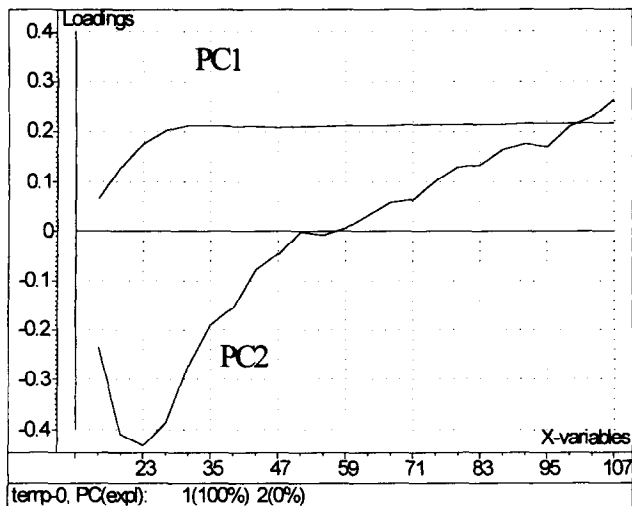


Fig. 7. Loadings of the FID points for PLS1 on water content. Abscissa values correspond to the time of measurements in  $\mu$ s.

by points around 23  $\mu$ s (Fig. 7). The plot of the scores (Fig. 8) shows that points around 23  $\mu$ s correspond to the samples where there is mobilization of the matrix as seen in Fig. 3 (inflection point) and in Fig. 6 (minimum).

These multivariate statistical analyses highlighted the different nature of the information contained in the  $T_1$  values and the significant change in the FID curves around 23  $\mu$ s.

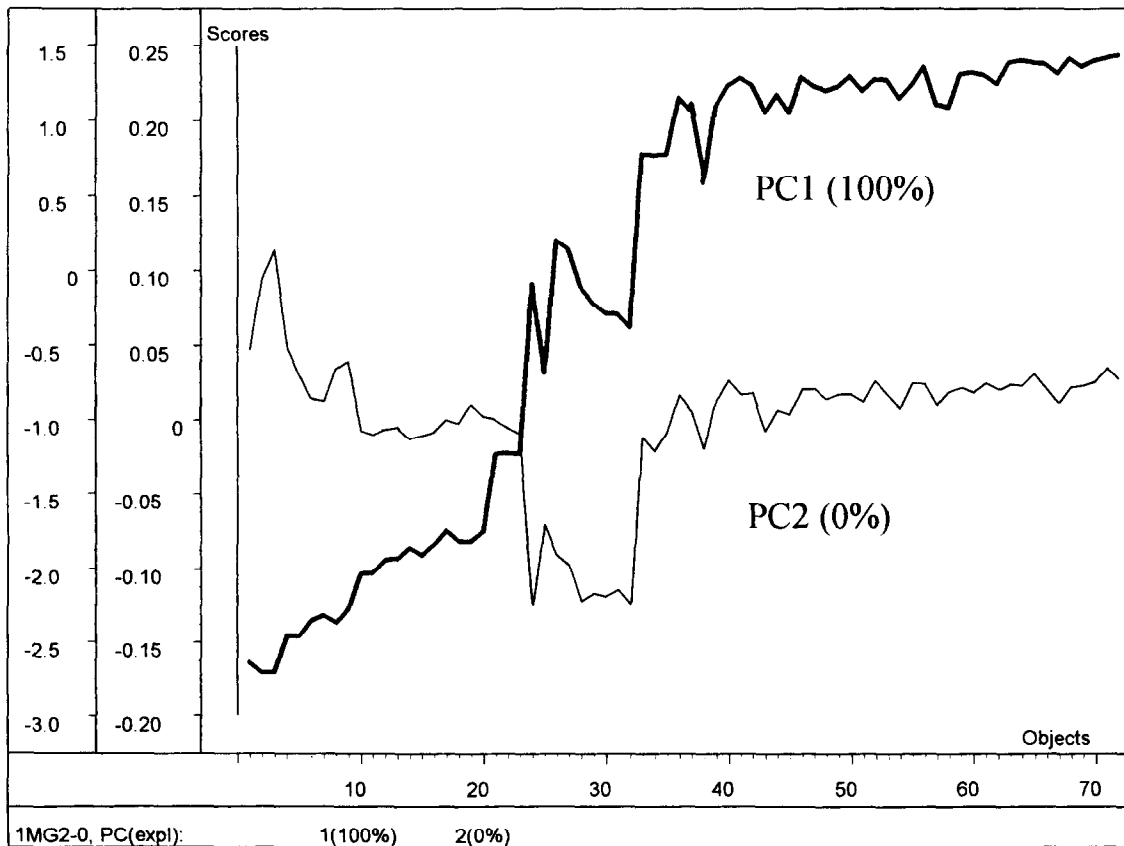


Fig. 8. Scores of the samples for PLS1 on water content. Objects are numbered in order of increasing water content.

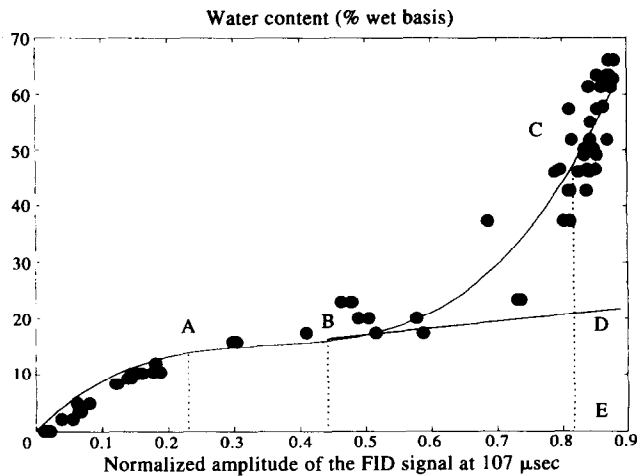


Fig. 9. Plot of the water content against the FID signal at 107  $\mu$ s.

After having shown that FID points were important parameters for the characterization of water, we plotted the water content against the FID signal intensities for the different points. The resulting curves (Fig. 9) all had shapes similar to the BET (Brunauer–Emmet–Teller) sorption isotherm model curves which are usually represented with the water content as ordinate and the water activity ( $A_w$ ) as abscissa (Brunauer *et al.*, 1938).

By analogy with the BET curves, five noteworthy points, representing different states of water in food, are indicated in Fig. 9. Point A is the inflexion point of the first part of the curve. Below this point (12.9% water), water has little mobility and is strongly adsorbed on the specific polar sites by hydrogen bonds to form a hydration monolayer which corresponds to the quantity of water that is just sufficient to saturate the polar groups of the gelatine. Between point A and point B, where a slope change takes place, water is moderately bound; this point, which marks the slope change, corresponds to 18.8% water. From then on, multimolecular layers begin to be filled. Above the critical point B, the water of the sample has the properties of a liquid, particularly its freezability. In this case, two fractions are observable: CD which represents the solvating properties of the sample and DE which corresponds to the zone where the water is strongly fixed by adsorption. DE is related to the quantity of non-solvating water in the product.

We propose the determination of BET curves and parameters by TD-NMR rather than by  $A_w$ . TD-NMR is faster and easier to use, so it should be possible to follow the evolution of a system that is not in equilibrium. Moreover, NMR parameters may be more directly related to the physical and the chemical characteristics of the samples.

## CONCLUSION

This paper shows that TD-NMR, whose advantages are numerous (non-destructive, simple, rapid measure-

ments, etc.), is a tool which is well adapted to the study of hydration.

This study also shows that multivariate statistical analyses may be very useful for the detection of significant variables. It also facilitates the extraction of hidden information, which can be of major importance in the interpretation of the results. In our case, it is of considerable help in the development of rapid methods for the prediction of water content and hydration state.

In the case of gelatine solutions, NMR parameters such as  $T_1$  (or  $R_1$ ),  $T_2$  (or  $R_2$ ), FID and  $M0_{src}/FID_{11}$  give much information concerning the dynamics of water:

1. The nature of the interactions (effect of pH and temperature on  $R_1$  and  $R_2$ ).
2. The hydration state, water mobility (FID,  $T_1$  and  $M0_{src}/FID_{11}$ ).
3. The detection of chemical exchange ( $R_2$  measurements with variable tau).

These parameters are very sensitive to changes in water content, and also water mobility. Some of them, such as the  $T_1$  and the ratio  $M0_{src}/FID_{11}$ , could be used as probes for the state of hydration of a given gelatine solution. Moreover, the TD-NMR measurement can replace the  $A_w$ , which is a very subjective notion whose determination is time-consuming and often difficult. This technique should therefore lead to important advances in our knowledge concerning the dynamics of water in biological products.

## ACKNOWLEDGEMENTS

The authors gratefully acknowledge funding from the I.N.R.A. (Institut National de la Recherche Agronomique).

## REFERENCES

- Belton, P. S. (1984). Nuclear magnetic resonance and photo-acoustic spectroscopy. In *Biophysical Methods in Food Research*, ed. H. W.-S. Chan. Blackwell Scientific, London, pp. 103–137.
- Brunauer, S., Emmett, P. H. & Teller, E. (1938). Adsorption of gases in multimolecular layers. *J. Am. Chem. Soc.*, **60**, 309–319.
- Carver, J. P. & Richard, R. E. (1972). A general two-site solution for the chemical exchange produced dependence of  $T_2$  upon the Carr–Purcell pulse sequence. *J. Magn. Reson.*, **6**, 89–105.
- Duckworth, R. B. (1975). *Water Relations in Foods*. Academic Press, London.
- Hills, B. P., Takacs, S. F. & Belton, P. S. (1990). A new interpretation of proton NMR relaxation time measurements of water in food. *Food Chem.*, **37**, 95–111.
- Marquardt, D. W. (1963). An algorithm for least-squares estimation of non linear parameters. *J. Soc. Ind. Appl. Math.*, **11**, 431–441.
- Monteiro Marques, J. P., Rutledge, D. N. & Ducauze, C. J. (1991). Low resolution pulse NMR detection of the mobilization point of solutes during the drying of carrots. *Lebensm. Wiss. Technol.*, **24**, 93–98.